Articles

Linear Low-Density Polyethylene Containing Precisely Placed Hexyl Branches

John C. Sworen and Kenneth B. Wagener*

The George and Josephine Butler Polymer Research Laboratory, Department of Chemistry, University of Florida, Gainesville, Florida 32611-7200

Received February 5, 2007; Revised Manuscript Received April 20, 2007

ABSTRACT: A structural investigation into model linear low-density polyethylene containing precise hexyl branches has been completed using metathesis chemistry. These models based on ethylene/1-octene (EO) copolymers are versions of industrially produced metallocene copolymers; however, they contain exact primary structures and constant methylene sequence lengths. Acyclic diene metathesis (ADMET) polymerization has been used to produce copolymers containing only hexyl branches on every 9th, 15th, or 21st carbon along the backbone of polyethylene. Thermal examination of these macromolecules has demonstrated the first narrow melting profile for EO copolymers with high 1-octene incorporation (111, 67, and 48 hexyl branches per 1000 carbons). Further, a new synthetic methodology has been developed to produce branched, pure diene functional monomers with the ability to produce any model LLDPE in good yields.

Introduction

Polymers based around the selective homopolymerization of ethylene or through its copolymerization with α-olefins have been produced for almost 60 years to manipulate linear polyethylene's base material properties.[1−8] Enhancements to the world's simplest macromolecule can be accomplished using numerous methods based on catalyst or initiator choices, chain transfer events, monomer types (or feed), reactivity ratios, or temperature and pressure variations. Overall, these events produce defects to alter the polymers stiffness, tensile strength, processability, and softening temperature due to changes in branch type and short chain branching distribution (SCBD).[9] The various types of copolymers can be classified into groups based on the nature or method of this "defect" incorporation. In the current polyolefin market, linear low-density polyethylene (LLDPE), the linear copolymers of ethylene, and an α-olefin offer enhanced behavior over all other structural versions of polyethylene. The widespread interest in LLDPE materials is due to the excellent combination of processability and good mechanical performance caused by their low densities and relative homogeneous linear backbones.

Commercial LLDPEs are produced using a multitude of systems based on either Ziegler−Natta or metallocene catalysts. The less effective Ziegler−Natta systems tend to favor high ethylene insertion rates, yielding ill-defined and heterogeneous primary structures.[10−12] Also, these systems tend to produce low-molecular-weight materials and high-molecular-weight distributions originating from the tendency to multisite initiate. In contrast to conventional Ziegler−Natta catalysts, single-site catalysts provide copolymers with narrower composition and molecular weight distributions and higher levels of comonomer incorporation.[13−21] Several researchers have shown that the coordination geometry of metallocenes plays an important role in the final structure of the copolymer.[22] In fact, the manipulation of such catalytic systems is often used to alter and vary the behavior of LLDPEs. Practical application of these systems has been the development of constrained geometry catalysts (CGC) based on *ansa*-monocyclopentadienylamido group 4 metal complexes; their high catalytic activity and ability to generate macromonomers have produced copolymers with excellent processability and mechanical properties.[20]

In recent years, the development of living polymerizations utilizing highly hindered late transition metal systems have yield well-defined copolymers through controlled chain walking. These new systems allow for controlled polymer microstructures from stock α-olefins using a chain-type polymerization mechanism. The polymer's microstructure can be tailored by both monomer choice (propylene, 1-butene, etc.) and ligand selection (bulkiness and symmetry), leading to varying branch concentrations and regioregularity.[23−26]

The plethora of LLDPEs synthesized using either metallocene or Ziegler−Natta systems have motivated research groups to study their behavior.[27−37] Regardless of the polymerization method, random errors introduce unavoidable defects causing molecular heterogeneity and hence heterogeneous structures. Overall, the documented average defect content in metallocene-synthesized polyolefins has been narrow. Reactivity variations still yield copolymers with locally heterogeneous structures due to uncontrollable insertion rates. Our approach in the study of ethylene-based copolymers has been based on organic synthesis. In this fashion, the primary structure of any LLDPE can be predetermined through the correct choice of macromonomers in contrast to indirect methods (catalyst and temperature), which

* Corresponding author. E-mail: wagener@chem.ufl.edu.

10.1021/ma070317k CCC: $37.00
Published on Web 05/25/2007

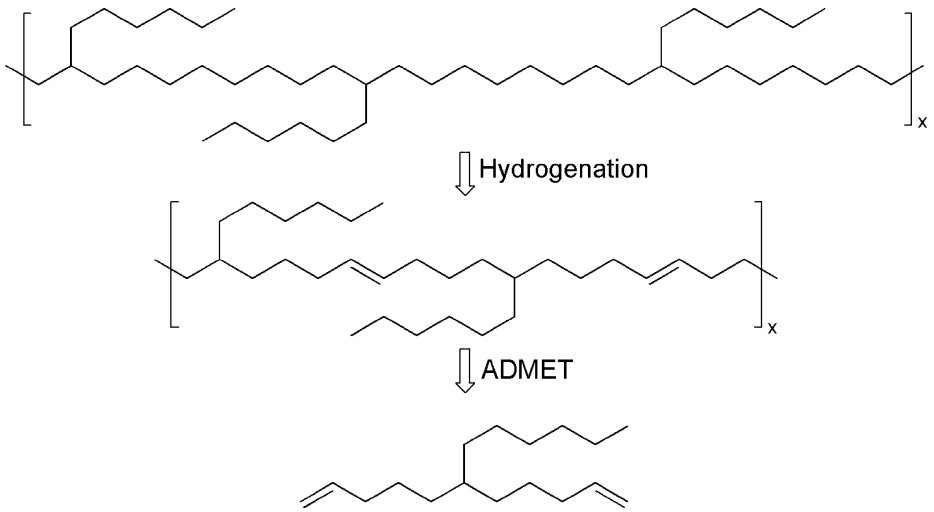

Figure 1. Modeling precisely branched ethylene/1-octene copolymers using organic methods.

tend to cause an additional level of encumbrance when studying systems based on a sole comonomer. Figure 1 demonstrates the retro-synthesis design using the clean, step polymerization chemistry offered by acyclic diene metathesis (ADMET) to produce compositionally precise LLDPEs, which are outlined for ethylene/1-octene owing to known branch identity and placement.

The first example of this methodology was the synthesis of five model ethylene/propylene (EP) copolymers in which the methyl branch was precisely placed on every 9th, 11th, 15th, 19th, or 21st carbon along the backbone, respectively.[38] Continuation of this research led to the development of structural homogeneous copolymers of ethylene and 1-butene (EB) containing symmetrically placed ethyl branches.[39] The copolymers produced using these methods have exhibited unique thermal and structural behavior—in effect, creating a new class of PE-based materials. In order to validate the behaviors observed in the precise studies, a series of random methyl branched polyethylenes were produced using ADMET copolymerization.[40] Through these initial studies it was concluded that the morphology of these model copolymers resulted solely from the precise control of primary structure in turn enabling access to never observed behavior.

We now report the polymer synthesis, characterization, and thermal analysis for our most recent attempt to produce LLDPEs as models for chain-addition copolymers of ethylene and 1-octene. The ADMET polymerization of the symmetrically hexyl-substituted monomers and their subsequent hydrogenation has yielded copolymers containing a hexyl on each and every 9th, 15th, or 21st carbon. The resulting ADMET copolymers are based on a linear polyethylene backbone without the influences from unwanted branch content, heterogeneous branch distributions, and interchain heterogeneity. Herein, we also present a universal synthesis to yield pure α,ω-diene monomers containing any length alkyl branch using commercially available alkyl bromides.

Results and Discussion

A. Monomer Synthesis and Characterization. The study of ethylene copolymers, largely their linear low-density analogues, has centered on chain-addition polymerization where the copolymer's architecture is modified by a selective choice of either transition metal, monomer type, or monomer feed control.[13−22,41−54] Our approach to investigate LLDPEs was to allow organic synthesis instead of indirect manipulation to modify the polymer's primary structure. The major advantage of this approach is the inherent ability to govern the copolymer's properties by the appropriate organic building block, resulting in a single repeating unit independent of catalyst choice or monomer feed ratios. Coupling the correct monomer synthesis with a consistent and error-free polymerization mechanism allows for the production of precise macromolecules.

In the past, monomer synthesis to consistently produce pure α-olefin functionality and branch purity has proven difficult. Numerous methodologies have been investigated to encompass both purity requirements.[38,39] Figure 2 illustrates a universal synthetic methodology with the ability to produce a variety of branch identities from a common starting material. The starting compounds used in this study were modified from an earlier published procedure by Wagener.[55] Starting from diethylmalonate, compound **6** was synthesized using sodium hydride and a respective bromoalkene, followed by decarboxylation of the resulting diacid. The monoacid was reduced to the primary alcohol and directly converted to the sulfonic acid ester (**8**) using mesyl chloride.

Using the above materials as a starting point, a detailed study centered on developing a universal coupling reaction to insert the branch functionality regardless of the starting alcohol. To add further utility, the use of a simple and inexpensive branch precursor was also investigated. Typically, the coupling of carbon moieties to existing structures is mediated via a transition metal complex, such as nickel or palladium, which tends to have high α-olefin binding affinities. These large binding rates compete with substitution, leading to olefin isomerization even with low metal concentrations (0.5 mol %). However, the combination of softer metals and lower temperatures essentiallly alleviates the unwanted olefin isomerization.

In the past, copper-based complexes have shown a wide range of utility in carbon−carbon bond formation from either the starting Grignard or lithium reagents and are softer than nickel or palladium. The most common routes are based on organocuprate (I) or Gilman reagents, R_2CuLi, which have shown highly selective substitutions with alkyl, alkenyl, and aryl halides or tosylates.[56−58] However, the available starting lithium reagents limit the production of Gilman complexes as well as the need for high excess of the organocuprate (500%) to achieve moderate yields. Also, "lower order" cuprates have difficulty in substitutions at highly hindered reaction centers. "Higher order" cuprates overcome these shortcomings but still at the expense of high catalyst loadings and the starting lithium reagent. The highly

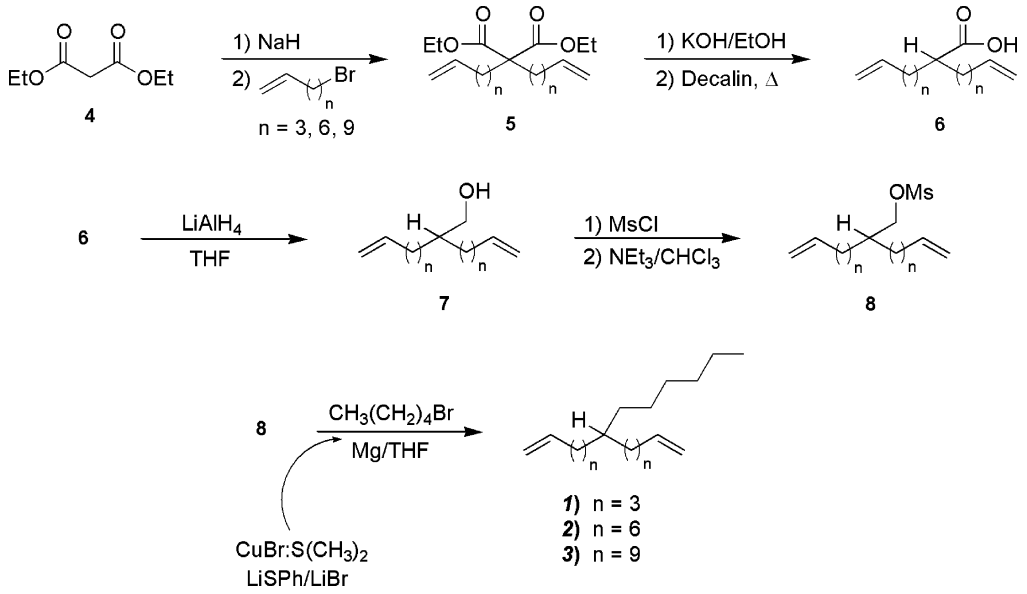

Figure 2. Synthetic method utilized to produce model EO monomers.

hindered reaction center in our monomers and the lack of commercially available lithium reagents resulted in an investigation into modifying and softening the basicity of Grignard reagents. One of the simplest, the addition of copper salts, yields Grignards having the ability to add in a conjugated or homoaddition mode with copper loadings as low as 1 mol %.[59] In fact, the addition of copper iodine to a solution of compound **8** with the respective alkyl magnesium reagent generated low yields (<5%) of the hexyl branched monomer with complete uptake of the starting mesylated alcohol. However, the conversion was to the reduced methyl branched monomer.

Two basic approaches can be used to alleviate this competing reduction mode of alkyl cuprates through the formation of heterocuprates. The fundamental idea is the addition of a nontransferable group aids in alkyl transfer and hinders the intermolecular reduction. These heterocuprates are produced through the bonding of copper with either a sp or sp^2 carbon (e.g., alkenyl or 2-thienyl) or the attachment of a heteroatom based ligand such as sulfur or nitrogen. In the past, Burns et al. have investigated the coupling of alkyl sulfonates with Grignard regents using highly efficient soluble thiocuprates.[60] A series of model reactions were performed to investigate the substrate effects encountered in the synthesis of our symmetrically positioned hexyl branched dienes. Overall, the optimal results were obtained using the mesylated-protected alcohol (**8**), 10 mol % of the cuprate, and the addition of HMPA with mild heating of the reaction mixture. The clean and efficient chemistry afforded using this system (illustrated in Figure 2), and the availability of starting alkyl magnesium reagents has expanded the scope of ADMET to model long chain branching in LLDPEs.

B. ADMET Polymerization and Hydrogenation Chemistry. In the past acyclic diene metathesis (ADMET) has been useful for the synthesis and modeling of perfectly branched polymer structures (Figure 3).[38,61] The mechanism of step-condensation metathesis offers control over molecular weight, polydispersity, branch identity, and branch frequency in the final material. Metathesis allows for complete conversion of the monomer functionality to the growing polymer chain without influences of chain transfer, which results in a purely linear PE backbone. As illustrated in Figure 3, ADMET produces high polymer from a metal mediated coupling of two terminal olefins driven by the condensation of ethylene. The consequence of

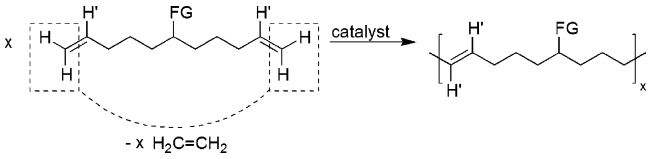

Figure 3. Acyclic diene metathesis (ADMET) polymerization.

this polymerization control allows for branch identity and type to be a function of monomer selection.

In this paper, the ADMET chemistry yields a linear, unsaturated polymer that is comprised of only one type of repeat unit, in addition to the usual amount of cyclics (<1−2%) found in bulk polycondensation conversions.[38,40,61] Metathesis, similar to all step-condensations, requires high monomer purity to obtain high conversion. The most effective methods have been outlined in the past, ultimately leading to monomers dried over metal mirrors. The polymerization proceeds efficiently using Schrock's catalyst (750:1 loading, monomer:catalyst)[62−67] followed by exhaustive hydrogenation over palladium on carbon (10 wt % Pd/C). The hydrogenations can be completed over 4 days and purified by precipitation in acidic methanol (1 M). The efficiency of hydrogenation can easily be quantified by infrared (IR) spectroscopy, gathered by observation of the out-of-plane alkene C−H bend, and NMR analysis.[40]

The molecular weights of the model copolymers are displayed in Table 1 and confirm that the ADMET prepolymer is not affected by the hydrogenation conditions employed. The decrease in the molecular weight data observed for LLALS was expected because of the difference in dilute solution behavior of PE vs PS, not due to scission of the polymer chains. Independent of determination method, the molecular weights for the ADMET EO copolymers are sufficiently high to model 1-octene LLDPEs, coinciding with earlier experiments.[38,40,61]

As with all metathesis generated model copolymers, nomenclature is based on the parent chain-addition copolymer. All copolymers begin with the prefix **HP** (hydrogenated polymer) followed by the comonomer type (**EO**, ethylene/1-octene) and the precise branch frequency (**21**); for example, **HPEO21** is designated as the hydrogenated ethylene/1-octene copolymer containing a hexyl branch on every 21st carbon. Because of the exact nature of the polymers produced, the comonomer content can be easily calculated using the branch frequency (*n*)

Table 1. Molecular Weights and Structural Data for ADMET Model EO Materials

		branch content per 1000 carbons[b,c]		$M_w \times 10^{-3}$ (PDI)[f]		
				unsaturated	saturated	
model EO copolymer	hexyl on every *n*th backbone carbon[a] *n*	methines[b]	hexyls	relative[d]	relative[d]	LALLS[e]
HPEO9	9	67	111	58.2 (1.8)	55.6 (1.7)	27.1 (1.8)
HPEO15	15	48	67	44.5 (1.8)	47.2 (1.8)	26.2 (1.8)
HPEO21	21	37	48	44.6 (1.8)	46.1 (1.7)	25.8 (1.8)

[a] Branch content based on the hydrogenated repeat unit. [b] Branch content measured as methines/1000 total carbons (include the branch carbons). [c] Branch content measured as hexyls/1000 backbone carbons (excluding the branch). [d] Molecular weight data taken in tetrahydrofuran (40 °C) relative to polystyrene standards. [e] Molecular weight data taken using low-angle laser light scattering (LALLS) in tetrahydrofuran at 40 °C. [f] Polydispersity index (M_w/M_n).

following the relationship

$$\text{mol \% comonomer} = \frac{2}{n} \times 100$$

In order to develop a better understanding of polyethylene behavior during crystallization, copolymers with high comonomer content were used to investigate the minimum methylene sequence length. Table 1 lists the branch content of the copolymers produced on the basis of the total number of carbons or backbone carbons alone. The polymers have exact primary structures and are the first examples of EO copolymers containing precisely placed hexyl branches on each 9th, 15th, or 21st carbon along polyethylene's linear backbone.

C. Structural Data. The ability to control a copolymer's primary structure allows for an opportunity to generate information on the macromolecular structure of any ethylene-based material. Metathesis is a useful tool to synthesize copolymers without the influences of chain transfer and heterogeneous comonomer incorporation. This unique control can be realized by examination of the ^{13}C NMR spectra of a monomer to copolymer transformation. Figure 4 shows the carbon spectra for an ADMET polymerization from monomer to unsaturated polymer followed by its complete hydrogenation to produce the model copolymer **HPEO9**. The solution behavior of these EO model copolymers tends to mimic previously synthesized ADMET LLDPEs, highly soluble in typical organic solvents used for polyolefin macromolecules. Comparisons to linear small molecules or methyl and ethyl branched copolymers indicate precise structures with distinct branch and main chain resonances.

The clean and complete nature illustrated in Figure 4 results from carbons observed for one polymeric repeat unit, typical of ADMET polymerizations. The spectral data support the formation of a single repeating unit as evident by the disappearance of the external olefins from monomer **1** (114 and 139 ppm) to a single cis:trans internal olefin observed at 129.9 and 130.3 ppm, respectively. Further, the ^{13}C NMR confirms the exhaustive hydrogenation by the lack of the internal sp^2 carbons found in the unsaturated polymer. Upon close inspection **HPEO9**'s repeating unit and the spectral data both consist of 11 different carbons. The model copolymers give the typical side chain hexyl branch resonances, specifically 14.4 ppm ($-CH_3$) and 23.0 ppm ($-CH_2CH_3$) along with the branch point carbon resonating at 37.7 ppm.

Further studies of these ADMET model EO copolymers were performed using infrared (IR) spectroscopy; the results are illustrated in Figure 5. In the past, Tashiro et al. carried out a study of branching behavior on polyethylene packing using wide-angle X-ray diffraction (WAXD) supplemented by infrared spectroscopy.[68] Detailed infrared studies on previous ADMET copolymers have revealed the same connections of interchain

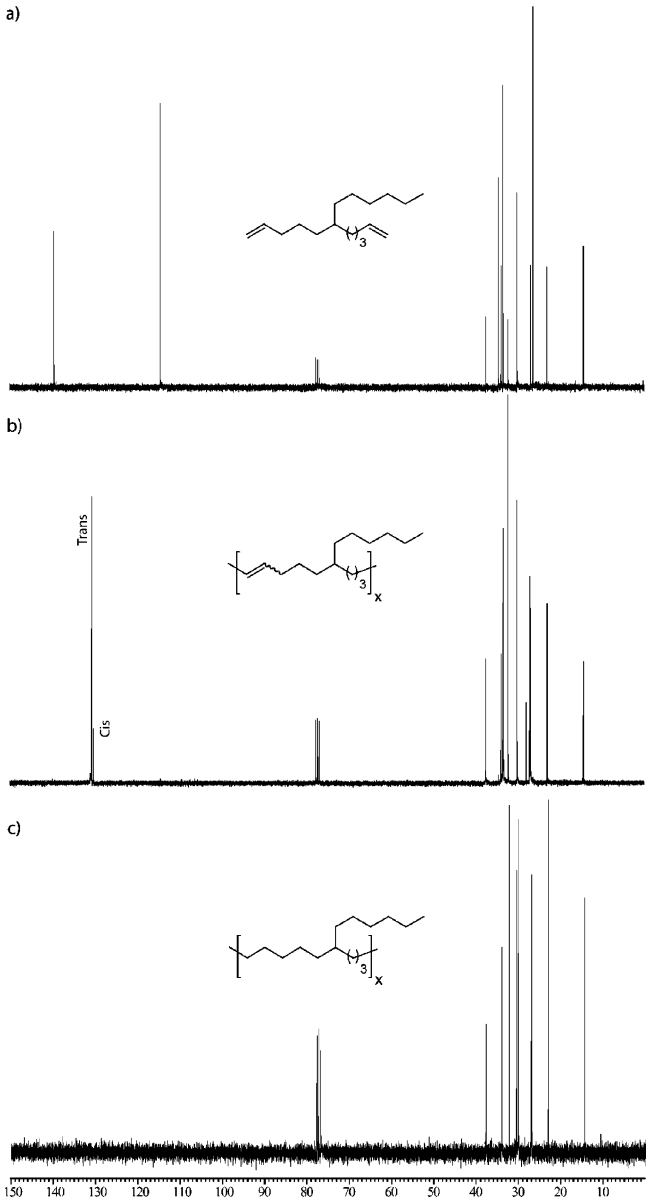

Figure 4. Comparison of ^{13}C NMR spectra for a typical ADMET polymerization transformation: (a) monomer **1**, (b) ADMET unsaturated prepolymer, and (c) **HPEO9**.

defects to crystal behavior and crystal packing.[68] Unfortunately, our ability to further compare the solid-state data gathered for these EO copolymers is limited due to the rather low melting points of either semicrystalline copolymer. However, detailed structural analysis can be made on the basis of well-defined absorbencies for the kink and double gauche defects following the 1366 cm^{-1} (1305 cm^{-1}) and 1352 cm^{-1} bands, respectively.

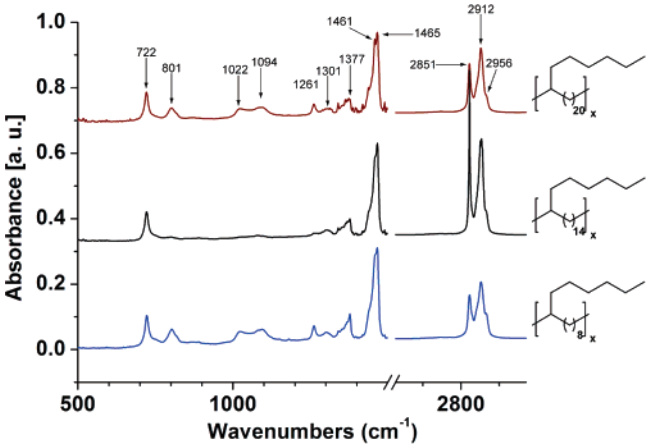

Figure 5. Infrared absorbencies for the ADMET model EO copolymers.

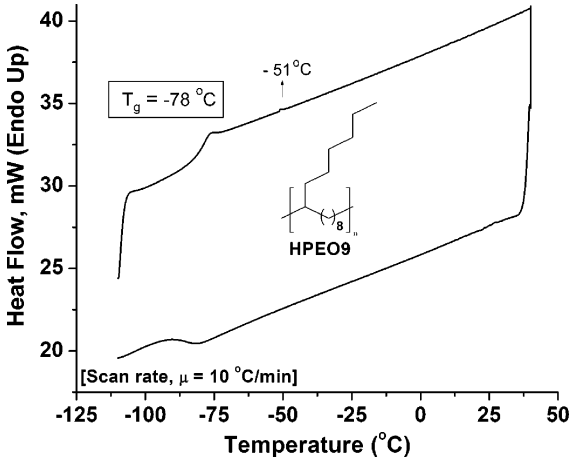

Figure 6. Thermal profile of the model EO copolymer containing a hexyl branch on each and every ninth backbone carbon, **HPEO9**.

In Figure 5, the IR spectra for the saturated ADMET EO copolymers are dominated by the two peak absorbencies observed for an unorganized packing structure. Moreover, the ADMET EO copolymers exhibit no signs of the characteristic absorbencies of an orthorhombic crystal or the symbolic Davidov splitting in the methylene rock region (~720 cm^{-1}). However, a faint doublet is witnessed in the methylene scissoring band (~1460 cm^{-1}) containing a broader lower wavenumber shoulder resulting from the highly distorted *trans*-polyethylene segments. Increasing the methylene sequence length causes the two distinct absorbencies (1461 and 1465 cm^{-1}) to become more defined, forgoing any influences to the methylene wagging band (722 cm^{-1}). The two experimental peaks at 722 and 1465 cm^{-1} have been assigned to a highly disordered phase; for example, a hexagonal phase has been observed in the previously synthesized ADMET copolymer containing a methyl group on every ninth backbone carbon.[38] Also, the additional observed scissoring absorbance at 1461 cm^{-1} and the accompanied shoulder are consistent with observation made in our detailed EB copolymer study.[39] Previously, the observed resonances have had separate origins in each copolymer series based on different branch incorporation mechanisms. The EO LLDPE series seems to cause the merging of these previously separate resonances despite the larger steric demand brought about by the precise hexyl branch. Interestingly, the larger defect volume does not seem to further alter either the methylene scissoring or wagging regions with the observed methylene wagging absorbance (722 cm^{-1}) being more consistent with the methyl copolymer series.

The IR bands at 1366 and 1305 cm^{-1} correspond to the 2g1 defect and can be easily quantified using infrared techniques. The overall concentration of this defect as well as the double gauche defect, observed at 1352 cm^{-1}, in the ADMET EO copolymers is constant regardless of methylene sequence length. This trend tends to follow the concentration of methyl end groups realized as an absorbance at 1377 cm^{-1} corresponding to the total branch concentration due to the polymer's high molecular weight. The longer methylene sequence lengths cause a broadening of these observed bands especially the 1301 cm^{-1} kink resonance when compared to our EB series. It should be noted that the EP copolymers do not exhibit these defect bands due to the methyl's incorporation into the growing crystal without the need for methylene rearrangement.

While at the present time the exact cause of these defects cannot be correlated to any secondary or higher order structure, comparisons tend to indicate that the copolymers contain high defect concentrations. These defects seem to correspond to branch concentrations independent of branch frequency. On the other hand, the highly branched copolymers contain two distinct methylene scissoring modes either deriving from main chain and side chain methylene vibrations or differing local environments. At the present time, it seems unlikely that the different vibrations are caused by methylene heterogeneity since the observed vibrations are common to short chain branched copolymers. In order to help elucidate the packing tendencies of our ADMET EO copolymers, a series of solid-state NMR experiments are currently underway. The initial study has been localized to **HPEO21** with hopes for further structural analysis using SAXS and WAXD.

D. Thermal Behavior. Commercial ethylene/1-octene (EO) copolymers constitute ~25% of the LLDPE market with numerous studies being performed on their thermal and material behavior annually.[41−54] Attempts to correlate initial monomer feed ratios to final material's responses are under investigation in order to develop structure/property functions to cost effectively mass-produce LLDPEs. Our goal is to develop a separate and fundamental understanding of the relationship between comonomers and branch frequency. The initial approach is to investigate the model copolymer's crystallization behavior and probe the crystallization kinetics of these new materials. Similar to the results obtained for our ADMET synthesized EP[38] or EB[39] copolymers, density, enthalpy, degree of crystallinity, and peak melting/recrystallization points all decrease as the amount of comonomer (1-octene) is increased.

Figure 6 shows the thermal profile for **HPEO9**, the model copolymer containing a hexyl branch on every ninth backbone carbon of polyethylene, suggesting a completely amorphous behavior. The data presented come as no surprise due to the short methylene sequences between branch points, resulting in small sequence lengths. In fact, the ADMET copolymer exhibits the exact same glass transition temperature (−78 °C) and behavior as for metallocene synthesized EO copolymers.[13−21] However, repeated DSC scans reveal a common and reproducible transition with an onset of −51 °C. It is unclear at this point whether the onset is either a melt transition based on small crystallizable regions or a second relaxation endotherm. For **HPEO9**, annealing experiments and heating rate variations seem to indicate the heat flow originates from a relaxational mode not semicrystallinity. It should be pointed out that a similar profile is commonly observed in semicrystalline branched chain-addition copolymers. Upon sample annealing the onset of the observed peak is unaltered. Moreover, a plot of molar branch

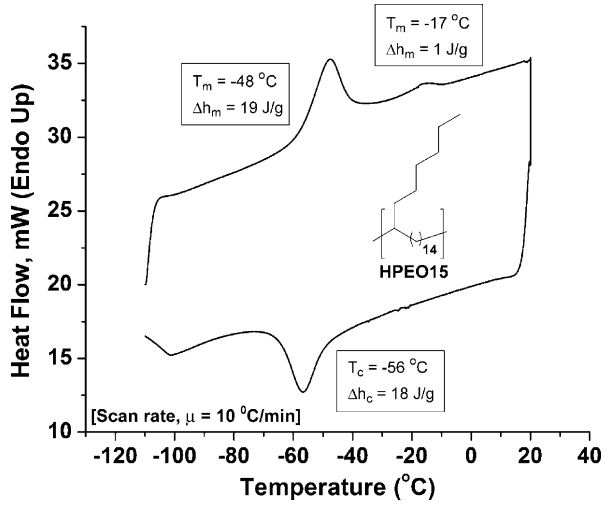

Figure 7. DSC melting and recrystallization thermograph for **HPEO15**.

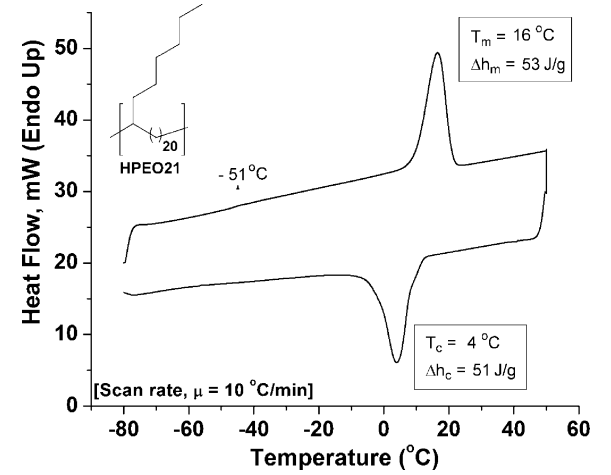

Figure 8. DSC melting and recrystallization thermograph for **HPEO21**.

content vs peak melting point, a complete series comparison to **HPEO15** and **HPEO21,** would suggest a melting point below that of the glass transition temperature.

The second model copolymer, **HPEO15**, turns out to exhibit semicrystalline nature, as illustrated in Figure 7. An increase in the methylene sequence length in turn produces a sharp and well-defined melting profile having a peak melting point of −48 °C. Also, at high sample loadings a second profile can be observed at −17 °C, owing to only a small fraction of the overall heat flow. It is uncertain whether this transition is caused by kinetic restraints brought out by its high concentration in the DSC pan or a second thicker crystal regime. Regardless of **HPEO15**'s melting profile, it is the first semicrystalline example of a precise melting EO copolymer containing high comonomer content (13−14%) and uniform methylene sequence length. Similar results have been observed for metallocene produced copolymers of ethylene and 1-octene with an average branch distribution centered on our ADMET content. It should be noted that the peak melting temperature in the metallocene samples is substantially higher (by ∼150 °C) with a considerable premelting region.

The initial attempt to synthesize and model ethylene/1-octene copolymers was completed by examination of **HPEO21**, producing the thermal profile shown in Figure 8. Similar to all previous model copolymers a sharp and well-defined endotherm is observed having a peak melting temperature of 16 °C. Unlike the previous copolymer **HPEO15**, the placement of a hexyl branch on every 21st carbon produces only a single melting peak. It is interesting to note the well-defined endotherm, lacking any visible premelting region, is similar to HDPE materials exhibiting little or no branch defects. In fact, the peak observed for **HPEO21** mimics the melting nature of our EP copolymer, **HPEP21**, albeit at a lower temperature. Of course, the thermal analysis of well-defined structures produces well-defined transitions. The heat flow for **HPEO21** is rather high (53 J/g) when compared to either the EP or EB coinciding with the previous **HPEB21** containing an ethyl branch on every 21st carbon.

It is also interesting to note the reappearance of the transition at −51 °C. It would seem that our precise hexyl branched polymer series show the same relaxation temperature independent of methylene length. Moreover, the transition seems to be common to all ADMET LLDPE materials and can be commonly observed in the majority of branched chain-addition copolymers. The transitions independence on sequence length and crystallinity indicates its correspondence to the β-relaxation produced by pendent side group motional relaxation. The consistent behavior of side group motion is not uncommon as they have also been observed to be independent of pressure effects in polypropylene, indicating main chain methylene segments act independently of side motion or their positional locale. Under the conditions used to monitor the thermal behavior of these copolymers, **HPEO9** yields two distinct relaxational pathways, reinforcing the idea of branch motional segregation.

Examination of the copolymers presented in this series and further comparisons to other ADMET models have brought about interesting questions. For example, the crystallization kinetics observed across the documented ADMET series shows unique trends. The crystallization kinetics observed for **HPEO15** seem to be unique to this class of ADMET copolymers. Comparisons to previously synthesized ADMET model EP and EB copolymers show different rates of supercooling dependent on branch type. In all cases the copolymers were examined under a cooling rate of 10 °C/min; however, the temperature differences between the peak melting and recrystallization endotherms gets narrower. The series following the trend **HPEP15**, **HPEB15**, and **HPEO15** have observed differences of 12, 10, and 8 °C, respectively. These differences may be realized by the formation of smaller crystallites and as a result faster recrystallization kinetics. On the other hand, comparisons of the 21st branch frequency copolymers do not reveal this trend. The data follow a 12, 18, and 11 °C temperature lag between the crystallization and recrystallization peaks for the copolymers **HPEP21**, **HPEB21**, and **HPEO21**. The observed differences may be a function of defect content or the longer run methylene run lengths produced by an increase in trans segments. Without further investigation, a complete change in crystal structure or morphology between **HPEO15** and **HPEO21** cannot be ruled out.

As indicated, thermal analysis seems to indicate small crystallite structures represented by the lower melting peaks when compared to the EP copolymer series;[38] however, the crystallization/recrystallization enthalpies seem to be completely nonuniform across the same series. Also, increasing the branch length when spanning the copolymers containing the same methylene sequences results in a distinct change of the characteristic melting peak following the apparent kinetic fluctuations observed during crystallization. The major distinction can be observed by the loss and reappearance of a well-defined endotherm when spanning the series (Figure 9). This trend is observed regardless of the frequency subset compared perhaps offering information about branch crystallization and

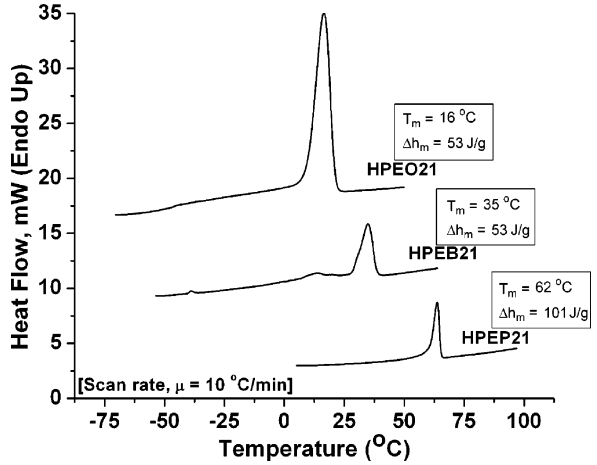

Figure 9. Thermal comparison of **HPEO21**, **HPEB21**, **and HPEP21**.

crystal incorporation. Figure 9 illustrates the calorimetric differences collected by keeping the branch frequency constant while systematically increasing the branch length.

Closer inspection of the entire ADMET copolymer series reveals that an increase in the side chain bulk produces inconsistent trends not easily understandable. The consensus that the majority of hexyl branches are excluded from crystallizing lamellae, and their higher free volume should suggest the observed spectra would tend to mimic the EB copolymers. However, this is not the case. As discussed previously, the thermal investigation of the precise EO copolymers tends to resemble and mimic the profiles obtained for the precise methyl branch series. The present data collection set favors partial hexyl branch inclusion particularly based on the thermal profiles. Of course, under equilibrium conditions the branches, even methyl, are assumed to be rejected from the growing crystallites.[69,70] Over the years, Flory's equilibrium theory has been modified to allow for short chain (methyl and ethyl) branch inclusion accounting for the collected experimental evidence.[69,70] Specifically, ethyl side groups have been thought to be on a boundary condition between inclusion and exclusion with segregation being a function of crystallization conditions. Up to this point there has been some debate whether larger branches, such has hexyl, could be included within the growing lamellae, favoring total branch exclusion.[71−73] Typically, studies have proposed interstitial sites along the polymer chain, known as kinks, which yield excess free volume allowing for branch incorporation. Arising from conformational gauche defects, the 2g1 is the most common defect proposed to be large enough for ethyl branches.[74−85] There has been some suggestion that larger defects can enter the crystal (<2%); however, there is no real experimental evidence for a 2g1 mechanism.

The melting point depression should not come as a surprise as this phenomenon is well documented, but the leveling of enthalpies can be observed regardless of branch bulkiness or frequency with the exclusion of methyl defects raises some questions. Also, the formation of well-defined thermal profiles for the EO copolymer series is interesting, having no comparison in either homogeneous metallocene or CGC systems produced by chain addition. As mentioned, throughout the study the ADMET EO copolymers resemble our EP copolymers, perhaps indicating some branch inclusion. The lack of density measurements, crystal structure data, and long spacing measurements for these ADMET EO polymers limits the correlations between branched models. However, formation of lamellae structures or any crystalline structure seems highly unlikely in **HPEO15** due to the small methylene sequence length and high concentration of trans segments without side chain involvement. The question of side chain self-crystallization can be ruled out since **HPEO9**, containing the highest concentration of branch defects, yields no melting endotherms in conjunction with only a single well-defined melting peak for **HPEO21**.

Conclusion

Acyclic diene metathesis polymerization has proven to control the primary structure of ethylene/1-octene copolymers, resulting in linear polyethylene containing only hexyl branches. In this effort, a simple synthetic method has been developed to produce exact linear model polymers of any short chain or long chain branching sequence. The inherent ability of metathesis to control the polymer's branch identity and placement has profound effects on the thermal and crystal behavior of these distinct EO materials, resulting in a new class of LLDPEs. The precise model EO copolymers tend to structurally mimic previously synthesized ADMET EP copolymers rather than our EB copolymers, specifically crystallization kinetics.

The structural investigation has shown that these ADMET EO copolymers seem to indicate side chain involvement in the crystallizing structures. Thermal analysis has indicated well-defined crystal structures albeit smaller when compared to metallocene structures while demonstrating a more homogeneous branching distribution over previously made EO copolymers. Moreover, these copolymers exhibit distorted methylene sequences with high concentrations of kink, gauche, and double gauche defects. We are currently continuing this branched polyethylene research by gathering a better base of scattering data and understanding the differences between random or commercial materials and precise branch content. In addition, we are investigating precisely branched linear low-density materials containing deuterated hexyl branches and attempting to locate and investigate molecular side chain motion. Ultimately, the syntheses of longer defects are underway with investigations into side chain cocrystallization and radically produced LDPEs.

Experimental Section

Instrumentation and Analysis. All ^{1}H NMR (300 MHz) and ^{13}C NMR (75 MHz) spectra were recorded on a Varian Associates Gemini 300 or Mercury 300 spectrometer. Chemical shifts for ^{1}H and ^{13}C NMR were referenced to residual signals from $CDCl_3$ (^{1}H = 7.27 ppm and ^{13}C = 77.23 ppm) with 0.03% v/v TMS as an internal reference. Reaction conversions and relative purity of crude reactions were monitored by chromatography and NMR. Gas chromatography (GC) was performed on a Shimadzu GC-17 gas chromatograph equipped with a 25 m capillary column packed with a 5% cross-linked PH ME and flame ionization detector. High-resolution mass spectral (LRMS and HRMS) data were obtained on a Finnegan 4500 gas chromatograph/mass spectrometer using the electron ionization (EI) mode. Elemental analyses were carried out by Atlantic Microlabs Inc., Norcross, GA.

Gel permeation chromatography (GPC) was performed using a Waters Associates GPCV2000 liquid chromatography system with its internal differential refractive index detector (DRI), internal differential viscosity detector (DP), and a Precision 2 angle light scattering detector (LS). The light scattering signal was collected at a 15° angle, and the three in-line detectors were operated in series in the order of LS−DRI−DP. The chromatography was performed at 45 °C using two Waters Styragel HR-5E columns (10 μm PD, 7.8 mm i.d., 300 mm length) with HPLC grade tetrahydrofuran as the mobile phase at a flow rate of 1.0 mL/min. Injections were made at 0.05−0.07% w/v sample concentration using a 322.5 μL injection volume. In the case of universal calibration, retention times were calibrated against narrow molecular weight polystyrene standards (Polymer Laboratories, Amherst, MA). All standards were

selected to produce M_p or M_w values well beyond the expected polymer's range. The Precision LS was calibrated using narrow polystyrene standard having an $M_w = 65\,500$ g/mol.

Fourier transform infrared (FT-IR) spectroscopy was performed using a Bio-Rad FTS-40A spectrometer. The hydrogenation of the unsaturated ADMET prepolymer was monitored by the disappearance of the out-of-plane C−H bend for the internal olefin at 967 cm^{-1}. Monomer was prepared by droplet deposition and sandwiched between two KCl salt plates. Unsaturated and hydrogenated polymer samples were prepared by solution-casting a thin film from tetrachloroethylene onto a KCl salt plate.

Differential scanning calorimetry (DSC) analysis was performed using a Perkin-Elmer DSC 7 equipped with a controlled cooling accessory (CCA-7) at a heating rate of 10 °C/min. Calibrations were made using indium and freshly distilled *n*-octane as the standards for peak temperature transitions and indium for the enthalpy standard. All samples were prepared in hermetically sealed pans (5−10 mg/sample) and were run using an empty pan as a reference and empty cells as a subtracted baseline.

Materials. Schrock's molybdenum catalyst $[(CF_3)_2CH_3CO]_2$(N-2,6-C_6H_3-*i*-Pr_2) Mo═CHC$(CH_3)_2$Ph was synthesized according to the literature procedure.[62−67] Tetrahydrofuran (THF) was freshly distilled from Na/K alloy using benzophenone as the indicator. The starting diethylmalonate and alkenyl bromides along with hexamethylphosphoramide and triethylamine were distilled over CaH_2. All other materials were used as received from the Aldrich Chemical Co.

General Monomer Synthesis. The following starting alcohols and their subsequent protection (modified to use methanesulfonyl chloride) were synthesized according to previously published procedures.[38,55] The characterization data for each protected alcohol are listed below.

In general, 224 mg (2.58 mmol) of LiBr and 530 mg (2.58 mmol) of CuBr·S$(CH_3)_2$ were added to a flame-dried, Ar-purged 100 mL round-bottom flask (RBF) equipped with a stir bar. The compounds were dissolved in 23 mL of dry THF. After stirring for 10 min, the flask was cooled to 0 °C, and 2.58 mL (2.58 mmol) of a 1 M lithium thiophenoxide (Aldrich) solution was added, producing a yellow complex. In a separate flame-dried three-neck RBF equipped with an additional funnel and stir bar, the mesylated alcohol ($n = 3$, 6, or 9 in Figure 2) was dissolved in THF:HMPA (3:1 v/v). This 1 M alcohol solution was cooled to 0 °C, and 10 mol % cuprate complex solution was added and stirred for 15 min. Pentylmagnesium bromide (1.5 equiv, 1 M in THF) was added dropwise over an hour, warmed to room temperature, and stirred for 24 h. Additional heating (30 °C) was required for good conversion of the longer methylene monomers. Workup was done by the addition of 100 mL of ether, extraction with 1 M HCl (100 mL) and saturated sodium chloride followed by drying over $MgSO_4$. The solution was filtered, concentrated, and purified by column chromatography using hexane. In addition, further purification was performed to remove any eliminated byproduct by distillation or reverse phase HPLC.

Characterization of 2-(Pent-4-enyl)hept-6-enyl Methanesulfonate (8a). Purification of compound **8a** yielded 98.2%.[38] The following spectral properties were observed: ^{1}H NMR ($CDCl_3$): δ (ppm) 1.20−1.50 (m, 8.5H), 1.62 (m, 0.5H), 2.05 (m, 4H), 3.00 (s, 3H), 4.12 (d, 2H), 4.96 (m, 4H, vinyl C***H***$_2$), 5.81 (m, 2H, vinyl C***H***). ^{13}C NMR ($CDCl_3$): δ (ppm) 26.75, 29.10, 29.90, 33.99, 37.42, 38.01, 72.7, 114.41 (vinyl ***C***H_2), 139.50 (vinyl ***C***H). EI/LRMS calcd for $C_{13}H_{24}O_3S$: 260; found: 260. Elemental analysis calcd for $C_{13}H_{24}O_3S$: 59.96 C, 9.29 H, 12.31 S; found: 59.6 C, 9.53 H, 12.01 S.

Characterization of 2-(Oct-7-enyl)dec-9-enyl Methanesulfonate (8b). Purification of compound **8b** yielded 99.2%.[38] The following spectral properties were observed: ^{1}H NMR ($CDCl_3$): δ (ppm) 1.20−1.50 (m, 20.5H), 1.62 (m, 0.5H), 2.05 (m, 4H), 3.00 (s, 3H), 4.12 (d, 2H), 4.96 (m, 4H, vinyl C***H***$_2$), 5.81 (m, 2H, vinyl C***H***). ^{13}C NMR ($CDCl_3$): δ (ppm) 26.75, 29.10, 29.24, 29.90, 30.87, 33.99, 37.42, 38.01, 72.7, 114.41 (vinyl ***C***H_2), 139.50 (vinyl ***C***H). EI/LRMS calcd for $C_{19}H_{36}O_3S$: 344; found: 344. Elemental analysis calcd for $C_{19}H_{36}O_3S$: 66.23 C, 10.53 H, 9.31 S; found: 66.01 C, 10.51 H, 8.99 S.

Characterization of 2-(Undec-10-enyl)tridec-12-enyl Methanesulfonate (8c). Purification of compound **8c** yielded 96.4%.[38] The following spectral properties were observed: ^{1}H NMR ($CDCl_3$): δ (ppm) 1.20−1.50 (m, 33.5H), 1.62 (m, 0.5H), 2.05 (m, 4H), 3.00 (s, 3H), 4.12 (d, 2H), 4.96 (m, 4H, vinyl C***H***$_2$), 5.81 (m, 2H, vinyl C***H***). ^{13}C NMR ($CDCl_3$): δ (ppm) 26.75, 29.10, 29.24, 29.55, 29.90, 29.99, 30.01, 30.87, 33.99, 37.42, 38.01, 72.7, 114.41 (vinyl ***C***H_2), 139.50 (vinyl ***C***H). EI/LRMS calcd for $C_{26}H_{50}O_3S$: 427; found: 427. Elemental analysis calcd for $C_{26}H_{50}O_3S$: 73.18 C, 13.64 H; found: 76.36 C, 13.58.

Synthesis and Characterization of 6-Hexyl-undeca-1,10-diene (1). Monomer **1** was synthesized as described above using the mesylated alcohol produced using 5-bromo-1-pentene. The crude monomer was purified using column chromatography (hexane) followed by fractional distillation (70 °C at 0.156 mmHg) to yield 67% of a colorless liquid. The following spectral properties were observed: ^{1}H NMR ($CDCl_3$): δ (ppm) 0.88 (t, 3H, −C***H***$_3$), 1.20−1.50 (m, 19H), 2.05 (m, 4H), 4.96 (m, 4H, vinyl C***H***$_2$), 5.81 (m, 2H, vinyl C***H***). ^{13}C NMR ($CDCl_3$): δ (ppm) 14.39 (−***C***H_3), 22.99, 26.31, 26.93, 30.07, 32.22, 33.41, 33.89, 34.51, 37.48, 114.41 (vinyl ***C***H_2), 139.50 (vinyl ***C***H). EI/HRMS calcd for $C_{17}H_{32}$: 236.2504; found: 236.2507. Elemental analysis calcd for $C_{17}H_{32}$: 86.36 C, 13.64 H; found: 86.36 C, 13.58 H.

Synthesis and Characterization of 9-Hexylheptadeca-1,16-diene (2). Monomer **2** was synthesized as described above using the mesylated alcohol produced using 8-bromo-1-octene. The crude monomer was purified using column chromatography (hexane) followed by fractional distillation (135 °C at 0.135 mmHg) to yield 62% of a colorless liquid. The following spectral properties were observed: ^{1}H NMR ($CDCl_3$): δ (ppm) 0.88 (t, 3H, −C***H***$_3$), 1.15−1.48 (m, 34H), 2.05 (q, 4H), 4.96 (m, 4H, vinyl C***H***$_2$), 5.81 (m, 2H, vinyl C***H***). ^{13}C NMR ($CDCl_3$): δ (ppm) 14.42 (−***C***H_3), 23.01, 26.95, 26.98, 29.28, 29.50, 30.13, 30.29, 32.26, 33.98, 33.99, 34.14, 37.69, 114.34 (vinyl ***C***H_2), 139.49 (vinyl ***C***H). EI/HRMS calcd for $C_{23}H_{44}$: 320.3443; found: 320.3446. Elemental analysis calcd for $C_{23}H_{44}$: 86.17 C, 13.83 H; found: 86.20 C, 13.82 H.

Synthesis and Characterization of 12-Hexyl-tricosa-1,22-diene (3). Monomer **3** was synthesized as described above using the mesylated alcohol produced using 11-bromo-1-undecene. The crude monomer was purified using column chromatography (hexane) to yield 59% of a colorless liquid. The following spectral properties were observed: ^{1}H NMR ($CDCl_3$): δ (ppm) 0.89 (t, 3H, −C***H***$_3$), 1.15−1.48 (m, 44H), 2.05 (q, 4H), 4.96 (m, 4H, vinyl C***H***$_2$), 5.81 (m, 2H, vinyl C***H***). ^{13}C NMR ($CDCl_3$): δ (ppm) 14.40 (−***C***H_3), 22.98, 26.96, 29.23, 29.44, 29.80, 29.91, 29.97, 30.11, 30.41, 32.24, 33.96, 34.09, 37.66, 114.24 (vinyl ***C***H_2), 139.42 (vinyl ***C***H). EI/HRMS calcd for $C_{29}H_{56}$: 404.4382; found: 404.4385. Elemental analysis calcd for $C_{29}H_{56}$: 86.05 C, 13.95 H; found: 86.17 C, 13.96 H.

General Polymerization Conditions. All glassware was thoroughly cleaned and flame-dried under vacuum prior to use. The monomers were dried over CaH_2 and K mirror and degassed prior to polymerization. All metathesis reactions were initiated in the bulk, inside an argon atmosphere glovebox. The monomers were placed in a 50 mL round-bottomed flask equipped with a magnetic Teflon stirbar. The flasks were then fitted with an adapter equipped with a Teflon vacuum valve. After addition of the catalyst, slow to moderate bubbling of ethylene was observed. The sealed reaction vessel was removed from the drybox and immediately placed on the vacuum line. The reaction vessel was then exposed to intermittent vacuum while stirring in an oil bath at 30 °C. Generally after 4 h, the polymerization was exposed to full vacuum ($<10^{-1}$ mmHg) for 24 h and then high vacuum ($<10^{-3}$ mmHg) for 96 h, gradually increasing temperature to 50 °C during the last 24 h of polymerization. The reaction vessel was then cooled to room temperature and exposed to air, and toluene was added. The mixture was heated to 80 °C in order to dissolve the resultant polymer and decompose any remaining active catalyst. The polymer/toluene

solution was taken up and precipitated dropwise into a vigorously stirred beaker containing 1500 mL of acidic methanol (1 M).

Polymerization of 6-Hexyl-undeca-1,10-diene (1) To Give UPEO9. Schrock's [Mo] catalyst (6.4 mg, 8.5×10^{-3} mmol) was added to monomer **1** (1.5 g, 6.3 mmol). Precipitation (−78 °C) yielded 1.3 g (88%) of a white, stringy material. ^{1}H NMR ($CDCl_3$): δ (ppm) 0.88 (t, 3H, methyl), 1.28 (m, br, 19H), 1.97 (m, br, 4H), 5.40 (m, br, 2H, internal olefin). ^{13}C NMR ($CDCl_3$): δ (ppm) 14.37, 22.96, 26.91, 26.98, 27.09, 27.90, 30.06, 32.21, 33.30, 33.44, 33.59, 33.88, 37.45, 130.15 (cis olefin), 130.62 (trans olefin). ^{13}C NMR ($CDCl_3$) integration of cis:trans peaks gives: 19:81. GPC data (THF vs polystyrene standards): M_w = 58 200 g/mol; PDI (M_w/M_n) = 1.8.

Polymerization of 9-Hexyl-heptadeca-1,16-diene (2) To Give UPEO15. Schrock's [Mo] catalyst (3.2 mg, 4.1×10^{-3} mmol) was added to monomer **2** (1.0 g, 3.1 mmol). Precipitation (−78 °C) yielded 0.95 g (95%) of a white, stringy material. ^{1}H NMR ($CDCl_3$): δ (ppm) 0.86 (t, 3H, methyl), 1.15−1.50 (m, br, 31H), 1.97 (m, br, 4H), 5.40 (m, br, 2H, internal olefin). ^{13}C NMR ($CDCl_3$): δ (ppm) 14.41, 23.05, 26.96, 27.52, 29.54, 29.66, 29.99, 30.10, 30.13, 30.31, 32.25, 32.93, 33.97, 37.68, 130.15 (cis olefin), 130.62 (trans olefin). ^{13}C NMR ($CDCl_3$) integration of cis:trans peaks gives: 14:86. GPC data (THF vs polystyrene standards): M_w = 44 500 g/mol; PDI (M_w/M_n) = 1.8.

Polymerization of 12-Hexyl-tricosa-1,22-diene (3) To Give UPEO21. Schrock's [Mo] catalyst (3.1 mg, 3.9×10^{-3} mmol) was added to monomer **3** (1.2 g, 2.9 mmol). Precipitation (−78 °C) yielded 1.1 g (96%) of a white, stringy material. ^{1}H NMR ($CDCl_3$): δ (ppm) 0.84 (t, 3H, methyl), 1.00−1.5 (m, br, 43H), 1.97 (m, br, 4H), 5.40 (m, br, 2H, internal olefin). ^{13}C NMR ($CDCl_3$): δ (ppm) 14.37, 22.97, 26.93, 26.98, 29.46, 29.60, 29.81, 29.94, 29.98, 30.05, 30.09, 30.42, 32.22, 32.87, 33.97, 37.68, 130.09 (cis olefin), 130.55 (trans olefin). ^{13}C NMR ($CDCl_3$) integration of cis:trans peaks gives: 16:84. GPC data (THF vs polystyrene standards): M_w = 44 600 g/mol; PDI (M_w/M_n) = 1.8.

General Hydrogenation Conditions. Hydrogenation was performed using a 150 mL Parr high-pressure stainless steel reaction vessel equipped with a glass liner and a Teflon stirbar. The unsaturated polymers were taken up in 75 mL of toluene and added to the glass liner with 1 equiv of 10% palladium on activated carbon. The glass liner was placed into the bomb and then sealed. The Parr vessel was purged with 150 psi (3×) of Grade 5 hydrogen gas (H_2) in order to minimize oxygen and water introduced from the atmosphere. The bomb was charged to 1000 psi, and the mixture was stirred for 24 h at 80 °C followed by 48 h at 100 °C. The resultant polymer was filtered and precipitated into acidic methanol (1 N stock solution prepared with HCl) to obtain a finely dispersed white solid. The polymer was filtered and transferred to a 50 mL round-bottom flask, evaporation under reduced pressure for 6 h, and further drying under high vacuum (3×10^{-4} mmHg) at 70 °C for 5 days.

Hydrogenation of UPEO9 To Give HPEO9. Precipitation yielded 0.800 g (90.7%) of a translucent, tacky material. ^{1}H NMR ($CDCl_3$): δ (ppm) 0.84 (t, 3H, methyl), 1.1−1.5 (br, 27H). ^{13}C NMR ($CDCl_3$): δ (ppm) 14.42, 23.01, 26.96, 27.03, 30.07, 30.14, 30.50, 32.26, 33.99, 34.00, 37.71. GPC data (THF vs polystyrene standards): M_w = 55 600 g/mol; PDI (M_w/M_n) = 1.7. DSC results glass transition temperature data: T_g = −78 °C, ΔC_p = 0.59 J/(g °C).

Hydrogenation of UPEO15 To Give HPEO15. Precipitation yielded 1.01 g (97.5%) of a white spongy material. ^{1}H NMR ($CDCl_3$): δ (ppm) 0.89 (t, 3H, methyl), 1.27 (br, 39H). ^{13}C NMR ($CDCl_3$): δ (ppm) 14.43, 23.03, 26.98, 27.02, 30.04, 30.14, 30.48, 32.27, 34.01, 37.70. GPC data (THF vs polystyrene standards): M_w = 47 200 g/mol; PDI (M_w/M_n) = 1.8. DSC results T_m (peak melting temperature) = −48 °C; Δh_m = 19 J/g; T_c (peak recrystallization temperature) = −56 °C; Δh_m = 18 J/g.

Hydrogenation of UPEO21 To Give HPEO21. Precipitation yielded 1.12 g (98.1%) of a white spongy material. ^{1}H NMR ($CDCl_3$): δ (ppm) 0.89 (t, 3H, methyl), 1.27 (br, 51H). ^{13}C NMR ($CDCl_3$): δ (ppm) 14.40, 22.99, 26.96, 26.99, 30.01, 30.12, 30.45, 32.24, 33.98, 37.67. GPC data (THF vs polystyrene standards): M_w = 46 100 g/mol; PDI (M_w/M_n) = 1.7. DSC results T_m (peak melting temperature) = 16 °C; Δh_m = 53 J/g; T_c (peak recrystallization temperature) = 4 °C; Δh_m = 51 J/g.

References and Notes

(1) Ke, B. *J. Polym. Sci.* **1962**, *61*, 47−59.
(2) Gutzler, F.; Wegner, G. *Colloid Polym. Sci.* **1980**, *258*, 776−778.
(3) Mirabella, F. M., Jr.; Ford, E. A. *J. Polym. Sci., Part B: Polym. Phys.* **1987**, *25*, 777−790.
(4) Alamo, R. G.; Mandelkern, L.; Stack, G. M.; Krönke, C.; Wegner, G. *Macromolecules* **1994**, *27*, 147−156.
(5) Pieski, E. T. In *Polyethylene*; Renfrew, A., Morgan, P., Eds.; Interscience Publishers: New York, 1960.
(6) Kim, Y.; Kim, C.; Park, J.; Kim, J.; Min, T. *J. Appl. Polym. Sci.* **1996**, *60*, 2469−2479 and references therein.
(7) Starck, P.; Malmberg, A.; Löfgren, B. *J. Appl. Polym. Sci.* **2002**, *83*, 1140−1156.
(8) Pak, J.; Wunderlich, B. *Macromolecules* **2001**, *34*, 4492−4503.
(9) Sun, T.; Brant, P.; Chance, R. R.; Graessley, W. W. *Macromolecules* **2001**, *34*, 6812−6820.
(10) Da Silva Filho, A. A.; Soares, J. B. P.; de Galland, G. B. *Macromol. Chem. Phys.* **2000**, *201*, 1226−1234.
(11) Takaoka, T.; Ikai, S.; Tamura, M.; Yano, T. *J. Macromol. Sci., Pure Appl. Chem.* **1995**, *A32*, 83−101.
(12) Czaja, K.; Białek, M. *Polymer* **2001**, *42*, 2289−2297.
(13) Madkour, T. M.; Gorderis, B.; Mathot, V. B. F.; Reynaers, H. *Polymer* **2002**, *43*, 2897−2908.
(14) Cheng, H. N. *Polym. Commun.* **1984**, *25*, 99−105.
(15) Suhm, J.; Schneider, M. J.; Mülhaupt, R. *J. Polym. Sci., Polym. Chem.* **1997**, *35*, 735.
(16) Schneider, M. J.; Mülhaupt, R. *J. Mol. Catal., Part A* **1995**, *101*, 11.
(17) Koivumäki, J. *Polym. Bull. (Berlin)* **1996**, *36*, 7−12.
(18) Li Pi Shan, C.; Soares, J. B. P.; Penlidis, A. *J. Polym. Sci., Polym. Chem.* **2002**, *40*, 4426−4451.
(19) Suhm, J.; Schneider, M. J.; Mülhaupt, R. *J. Mol. Catal., Part A* **1998**, *128*, 215−227.
(20) Wang, W.-J.; Kolodka, E.; Zhu, S.; Hamielec, A. E.; Kostanski, L. K. *Macromol. Chem. Phys.* **1999**, *200*, 2146−2151.
(21) Quijada, R.; Dupont, J.; Miranda, M. S. L.; Scripioni, R. B.; Galland, G. B. *Macromol. Chem. Phys.* **1995**, *196*, 3391−4000.
(22) Kasi, R. M.; Coughlin, E. B. *Organometallics* **2003**, *22*, 1534−1539.
(23) Rose, J. M.; Cherian, A. E.; Coates, G. W. *J. Am. Chem. Soc.* **2006**, *128*, 4186−4187.
(24) Fan, W.; Waymouth, R. M. *Macromolecules* **2001**, *34*, 8619−8625.
(25) Leatherman, M. D.; Brookhart, M. *Macromolecules* **2001**, *34*, 2748−2750.
(26) Cherian, A. E.; Lobkousky, E. B.; Coates, G. W. *Chem. Commun.* **2003**, 2566−2567.
(27) Vanden Eynde, S.; Rastogi, S.; Mathot, V. B. F.; Reynaers, H. *Macromolecules* **2000**, *33*, 9696−9704.
(28) Zhang, F.; Liu, J.; Xie, F.; Fu, Q.; He, T. *J. Polym. Sci., Polym. Phys.* **2002**, *40*, 822−830.
(29) Vanden Eynde, S.; Mathot, V. B. F.; Koch, M. H. J.; Reynaers, H. *Polymer* **2000**, *41*, 4889−4900.
(30) Androsch, A.; Wunderlich, B. *Macromolecules* **2000**, *33*, 9076−9089.
(31) Mathot, V. B. F.; Pijpers, M. F. J. *J. Appl. Polym. Sci.* **1990**, *39*, 979−994.
(32) Van Miltenburg, J. C.; Mathot, V. B. F.; van Ekeren, P. J.; Ionescu, L. D. *J. Therm. Anal. Calorim.* **1999**, *56*, 1017−1023.
(33) Wagner, J.; Phillips, P. J. *Polymer* **2001**, *42*, 8999−9013.
(34) Isasi, J. R.; Haigh, J. A.; Graham, J. T.; Mandelkern, L.; Alamo, R. G. *Polymer* **2000**, *41*, 8813−8823.
(35) Hay, J. N.; Zhou, X.-Q. *Polymer* **1993**, *34*, 1002−1005.
(36) Hosoda, S.; Nomura, H.; Gotoh, Y.; Kihara, H. *Polymer* **1990**, *31*, 1999−2005.
(37) Russell, K. E.; Hunter, B. K.; Heyding, R. D. *Eur. Polym. J.* **1993**, *29*, 211−217.
(38) Smith, J. A.; Brzezinska, K. R.; Valenti, D. J.; Wagener, K. B. *Macromolecules* **2000**, *33*, 3781−3794.
(39) Sworen, J. C.; Smith, J. A.; Berg, J. M.; Wagener, K. B. *J. Am. Chem. Soc.* **2004**, *126*, 11238−11246.
(40) Sworen, J. C.; Smith, J. A.; Wagener, K. B.; Baugh, L. S.; Rucker, S. P. *J. Am. Chem. Soc.* **2003**, *125*, 2228−2240.
(41) Mirabella, F. M. *J. Polym. Sci., Polym. Phys.* **2001**, *39*, 2800−2818.
(42) Ziegler, K. *Kunststoffe* **1955**, *45*, 506.
(43) Ziegler, K. Belg. Pat. 533,326, May 5, 1955.
(44) James, D. E. *Ethylene Polymers: Encyclopedia of Polymer Science and Engineering*, 2nd ed.; Wiley-Interscience: New York, 1986; p 329.
(45) Rix, F.; Brookhart, M. *J. Am. Chem. Soc.* **1995**, *117*, 1137−1138.

(46) Schmidt, G. F.; Brookhart, M. *J. Am. Chem. Soc.* **1985**, *107*, 1443−1444.
(47) Kim, J. S.; Pawlow, J. H.; Wojcinski, L. M., II.; Murtuza, S.; Kacker, S.; Sen, A. *J. Am. Chem. Soc.* **1998**, *120*, 1932−1933.
(48) Johnson, L. K.; Killian, C. M.; Brookhart, M. *J. Am. Chem. Soc.* **1995**, *117*, 6414−6415.
(49) Johnson, L. K.; Killian, C. S.; Author, S. D.; Feldman, J.; McCord, E. F.; McLain, S. J.; Kreutzer, K. A.; Bennett, M. A.; Coughlin, E. B.; Ittel, S. D.; Parthasarathy, A.; Tempel, D. J.; Brookhart, M. S. Int. Pat. Appl. WO96/23010, 1996.
(50) Union Carbide Japanese Patent 54-148093, 1979.
(51) Kaminsky, W.; Hähnsen, H.; Külper, K.; Wöldt, R. U.S. Patent 4542199, 1985.
(52) Eynde, S. V.; Mathot, V.; Koch, M. H. J.; Reynaers, H. *Polymer* **2000**, *41*, 3437−3453.
(53) Rachapudy, H.; Smith, G. G.; Raju, V. R.; Graessley, W. W. *J. Polym. Sci., Polym. Phys.* **1979**, *17*, 1211.
(54) Rangwala, H. A.; Dalla Lana, I. G.; Szymura, J. A.; Fiedorow, R. M. J. *Polym. Sci., Polym. Chem.* **1996**, *34*, 3379−3387.
(55) Hopkins, T. E.; Wagener, K. B. *Macromolecules* **2004**, *37*, 1180−1189.
(56) Posner, G. H.; Whitten, C. E; Sterling, J. J. *J. Am. Chem. Soc.* **1973**, *95*, 7788−7800.
(57) Bertz, S. H.; Eriksson, M.; Miao, G.; Snyder, J. P. *J. Am. Chem. Soc.* **1996**, *118*, 10906−10907.
(58) Johnson, C. R.; Dutra, G. A. *J. Am. Chem. Soc.* **1973**, *95*, 7777−7782.
(59) Dieter, R. K.; Silks, L. A.; Fishpaugh, J. R.; Kastner, M. E. *J. Am. Chem. Soc.* **1985**, *107*, 4679−4692.
(60) Burns, D. H.; Miller, J. D.; Chan, H.−K.; Delaney, M. O. *J. Am. Chem. Soc.* **1997**, *119*, 2125−2133.
(61) O'Gara, J. E.; Wagener, K. B.; Hahn, S. F. *Makromol. Chem., Rapid Commun.* **1993**, *14*, 657−662.
(62) Schrock, R. R.; Murdzek, J. S.; Bazan, G. C.; Robbins, J.; Dimare, M.; O'Regan, M. *J. Am. Chem. Soc.* **1990**, *112*, 3875−3886.
(63) Bazan, G. C.; Khosravi, E.; Schrock, R. R.; Feast, W. J.; Gibson, V. C.; O'Regan, M. B.; Thomas, J. K.; Davis, W. M. *J. Am. Chem. Soc.* **1990**, *112*, 8378−8387.
(64) Bazan, G. C.; Oskam, J. H.; Cho, H. N.; Park, L. Y.; Schrock, R. R. *J. Am. Chem. Soc.* **1991**, *113*, 6899−6907.
(65) Fox, H. H.; Schrock, R. R. *Organometallics* **1992**, *11*, 2763−2765.
(66) Feldman, J.; Murdzek, J. S.; Davis, W. M.; Schrock, R. R. *Organometallics* **1989**, *8*, 2260−2265.
(67) Oskam, J. H.; Schrock, R. R. *J. Am. Chem. Soc.* **1992**, *114*, 7588−7590.
(68) Tashiro, K.; Sasaki, S.; Kobayashi, M. *Macromolecules* **1996**, *29*, 7460−7469.
(69) Flory, P. J. *Trans. Faraday Soc.* **1955**, *51*, 848−857.
(70) Flory, P. J. *J. Chem. Phys.* **1949**, *17*, 223.
(71) McFaddin, D. C.; Russell, K. E.; Wu, G.; Heyding, R. D. *J. Polym. Sci., Polym. Phys.* **1993**, *31*, 175−183.
(72) McFaddin, D. C.; Russell, K. E.; Kelusky, E. C. *Polym. Commun.* **1986**, *27*, 204−206.
(73) Litvinov, V. M.; Mathot, V. B. F. *Solid State Nucl. Magn. Reson.* **2002**, *22*, 218−234.
(74) Pechhold, W. *Kolloid Z. Z.* **1968**, *228*, 1−38.
(75) Baltá-Calleja, F.-J.; Gonzalez Ortega, J. C.; Martinez de Salazar, J. *Polymer* **1978**, *19*, 1094.
(76) Heink, M.; Häberle, K.-D.; Wilke, W. *Colloid Polym. Sci.* **1991**, *269*, 675−681.
(77) Seguela, R.; Rietsch, F. *J. Polym. Sci., Lett.* **1986**, *24*, 29−33.
(78) Vonk, C. G. *J. Polym. Sci.* **1972**, *38*, 429−435.
(79) Kortleve, G.; Tuijnman, C. A. F.; Vonk, C. G. *J. Polym. Sci., Part A-2* **1972**, *10*, 123−131.
(80) Vonk, C. G.; Pijpers, A. P. *J. Polym. Sci., Polym. Phys.* **1985**, *23*, 2517−1537.
(81) Wunderlich, B. *Crystal Structure, Morphology, and Defects. Macromolecular Physics*; Academic Press: New York, 1973; Vol. 1.
(82) Gaucher, V.; Séguéla, R. *Polymer* **1994**, *35*, 2049−2055.
(83) Martinez de Salazar, J.; Baltá-Calleja, F.-J. *J. Cryst. Growth* **1980**, *48*, 283.
(84) Scherr, H.; Pechhold, W.; Blasenbrey, S. *Kolloid Z. Z.* **1970**, *238*, 396−405.
(85) Baltá-Calleja, F.-J.; Hosemann, R. *J. Polym. Sci., Polym. Phys.* **1980**, *18*, 1159−1165.

MA070317K